MOLECULAR AND CELLULAR BIOLOGY, Jan. 1993, p. 144–154
0270-7306/93/010144-11$02.00/0

Vol. 13, No. 1

RNA B Is the Major Nucleolar Trimethylguanosine-Capped Small Nuclear RNA Associated with Fibrillarin and Pre-rRNAs in *Trypanosoma brucei*

TOINETTE HARTSHORNE* AND NINA AGABIAN

Intercampus Program in Molecular Parasitology, School of Pharmacy, University of California, San Francisco, California 94143-1204

Received 19 March 1992/Returned for modification 6 May 1992/Accepted 9 October 1992

RNA B is one of three abundant trimethylguanosine-capped U small nuclear RNAs (snRNAs) of *Trypanosoma brucei* which is not strongly identified with other U snRNAs by sequence homology. We show here that RNA B is a highly diverged U3 snRNA homolog likely involved in pre-rRNA processing. Sequence identity between RNA B and U3 snRNAs is limited; only two of four boxes of homology conserved between U3 snRNAs are obvious in RNA B. These are the box A homology, specific for U3 snRNAs, and the box C homology, common to nucleolar snRNAs and required for association with the nucleolar protein, fibrillarin. A 35-kDa *T. brucei* fibrillarin homolog was identified by using an anti-*Physarum* fibrillarin monoclonal antibody. RNA B and fibrillarin were localized in nucleolar fractions of the nucleus which contained pre-rRNAs and did not contain nucleoplasmic snRNAs. Fibrillarin and RNA B were precipitated by scleroderma patient serum S4, which reacts with fibrillarins from diverse organisms; RNA B was the only trimethylguanosine-capped RNA precipitated. Furthermore, RNA B sedimented with pre-rRNAs in nondenaturing sucrose gradients, similarly to U3 and other nucleolar snRNAs, suggesting that RNA B is hydrogen bonded to rRNA intermediates and might be involved in their processing.

Two distinct classes of small nuclear RNAs (snRNAs) reside in the eukaryotic nucleus and are involved in processing and maturation of RNAs (5). One class, the nucleoplasmic snRNAs, includes five of the six most abundant snRNAs found in metazoan and yeast nuclei: U1, U2, U4, U5, and U6 snRNAs. Small nuclear ribonucleoprotein (snRNP) particles contain the nucleoplasmic snRNAs, core proteins which include the conserved Sm antigens recognized by sera from lupus patients, and additional particle-specific proteins. Together with pre-mRNAs, these snRNP particles assemble into spliceosome complexes in which introns are removed and exons are spliced together. Other, less abundant nucleoplasmic snRNPs are also involved in aspects of mRNA biogenesis; the U7 snRNP is implicated in 3′ end formation of histone pre-mRNA, and the U11 snRNP functions in polyadenylation.

The second class of snRNAs encompasses the nucleolar snRNAs (12, 49) and contains U3, one of the six abundant nuclear snRNAs of metazoan and yeast nuclei. Nucleolar snRNAs are associated with a highly conserved nucleolar protein, fibrillarin, which is precipitated from an evolutionarily diverse range of organisms by autoimmune antibodies produced in scleroderma patients (21, 28, 32, 41, 42). The nucleolar snRNAs are believed to have roles in rRNA processing, since the nucleolus is the site of ribosome biogenesis and since nucleolar snRNAs hydrogen bond with pre-rRNAs (11, 17, 36, 49). The U3 snRNA has been implicated in processing of the primary pre-rRNA transcript which contains 18S, 5.8S, and 28S rRNA sequences separated by internal transcribed spacers (ITS) and flanked by external transcribed spacers (ETS). Processing of the pre-rRNA commences with a cleavage in the 5′ ETS region in mammals, an event which may be conserved in all eukaryotes (12). Interactions between U3 snRNA and the 5′ ETS have been detected in vivo by psoralen cross-linking of RNAs in mammalian and yeast cells (4, 30, 47). A requirement for U3 snRNA in the primary cleavage of mammalian pre-rRNA has been demonstrated in vitro in mouse cell extracts (25). Additionally, in vivo depletion studies have shown that U3 snRNA is necessary for cleavage at the ITS1/5.8S border in *Xenopus* cells (41) and for multiple cleavages of yeast pre-rRNAs which culminate in 18S maturation (19). In yeast cells, the nucleolar U14 and snr10 snRNAs and fibrillarin have also been shown to affect pre-rRNA processing (29, 48, 50).

The trypanosomatids are protozoan parasites which represent an ancient lineage in the evolution of the eukaryotes. RNA metabolism in these organisms has several unusual characteristics, including the addition, by *trans* splicing, of a 5′ 39-nucleotide (nt) spliced leader (SL) sequence to all nuclear mRNAs (1, 27). Three U snRNAs that are required for *trans* splicing have been identified in *Trypanosoma brucei* (54); these are homologs of the U2, U4, and U6 snRNAs (31, 52, 53). These U snRNAs differ from those found in higher eukaryotes in that they are smaller in size, they do not encode an Sm consensus binding site, and the protein components of their snRNP particles are not recognized by antibodies against the conserved Sm antigens. Neither U1 nor U5 snRNA equivalents have been found in *T. brucei*.

A fourth abundant U snRNA, RNA B, was identified in *T. brucei* (31). This RNA was not clearly related to known snRNAs by sequence homology, and thus its identity and function were uncertain. It was postulated that RNA B might represent a highly diverged U1, U3, or U5 snRNA or might be a unique snRNA component of the *trans* splicing machinery. RNA B has a trimethylguanosine (TMG) cap structure and therefore is likely to reside in the nucleus and function in

* Corresponding author.

RNA processing as do all other characterized TMG-capped RNAs.

In this report, we present data which indicate that RNA B is a divergent homolog of U3 snRNA. Regions of homology with U3 snRNA, including a putative protein binding sequence conserved among snRNAs which associate with the nucleolar protein fibrillarin, are noted. The *T. brucei* fibrillarin was identified as a 35-kDa polypeptide which fractionated with RNA B and pre-rRNA in nucleolar preparations. Both RNA B and fibrillarin were immunoprecipitated by autoimmune antifibrillarin antibodies. RNA B was identified as the only TMG-capped RNA of trypanosomes which could be immunoprecipitated with this serum. RNA B also fractionated with pre-rRNA precursors on nondenaturing sucrose gradients, suggesting a hydrogen-bonded association with pre-rRNAs and a role in rRNA processing.

MATERIALS AND METHODS

Cellular fractionation. A pellet of 10^{10} log-phase procyclic *T. brucei* 427 RB cells was suspended in 5 ml of hypotonic buffer (10 mM *N*-2-hydroxyethylpiperazine-*N'*-2-ethanesulfonic acid [HEPES; pH 7.9], 1.5 mM $MgCl_2$, 10 mM KCl, 0.5 mM dithiothreitol [DTT], pepstatin [1 μg/ml], leupeptin [5 μg/ml], phenylmethylsulfonyl fluoride [20 μg/ml], RNAsin [0.1 U/ml]); cells were allowed to swell on ice for 10 min and were then disrupted in the presence of 0.2% Nonidet P-40 (NP-40) by 20 strokes in a Dounce homogenizer. Nuclei, effectively released from broken cells by this treatment as determined by 4',6-diamidino-2-phenylindole imaging, were pelleted through a 3-ml cushion of 0.8 M sucrose and 0.5 mM $MgCl_2$ by centrifugation at 8,000 × *g* for 10 min. The nuclei were fractionated into nucleoplasmic fractions (38, 55) by suspending the nuclear pellet in 2.5 ml of 0.35 M sucrose–0.5 mM $MgCl_2$ and sonicating the suspension at low setting for four pulses of 20 s each until no nuclear structures were obvious by microscopy. Sonic extracts were then layered over a 2.5-ml cushion of 0.88 M sucrose–0.5 mM $MgCl_2$ and centrifuged at 2,500 × *g* for 10 min. The upper two-thirds of the gradient was considered the nucleoplasm, and the pellet was considered the nucleolar fraction.

Immunoprecipitations. Whole cell extracts were prepared from procyclic *T. brucei* cells, which were grown to a density of approximately 1×10^7 to 2×10^7 cells per ml, harvested by centrifugation at 1,000 × *g* for 10 min, and washed once in a buffer composed of 30 mM HEPES (pH 7.9), 150 mM NaCl, 10 mM KCl, and 5% sucrose. The cell pellet was suspended in hypotonic buffer (see above) to a density of 10^9 cells per ml, sonicated at low setting for two bursts of 20 s each, adjusted to 0.05% NP-40 and 200 mM NaCl, and sonicated for two more bursts. The broken cells were incubated at 4°C with shaking for 20 min, and then cellular debris was removed by centrifugation at 16,000 × *g* for 20 min. The extract was used immediately for immunoprecipitation.

Immunoprecipitations were performed by binding approximately 100 μg of immunoglobulin G (IgG) to 25 ml of protein A-agarose beads (GIBCO BRL) at 4°C for 2 h and then washing the beads six times with 1 ml of NET200 buffer (200 mM NaCl, 50 mM Tris-HCl [pH 7.4], 0.05% NP-40). An amount of extract equivalent to 2×10^8 to 4×10^8 cells was incubated with the beads at 4°C for 2 h, and then the bound immunoprecipitated complexes were washed 10 times with 1 ml of NET200 buffer. Immunoprecipitations of purified RNAs were performed similarly except that *Escherichia coli* 16S and 23S rRNAs (50 μg/ml) were included during the immunoprecipitation as carrier.

Separation of hydrogen-bonded RNAs on nondenaturing sucrose gradients. Procyclic *T. brucei* cells were lysed in a buffer containing 100 mM sodium acetate, 5 mM magnesium acetate, 50 mM Tris-acetate (pH 7.9), 10 mM DTT, 0.5% NP-40, and 10 mM vanadyl ribonucleoside complex, adjusted to 2% sodium dodecyl sulfate (SDS) and 2 mg of proteinase K per ml, and incubated at 14°C for 15 min. The lysate was then cleared at 30,000 × *g* for 30 min, and RNAs were sedimented through a 10 to 30% sucrose gradient for 16 h at 60,000 × *g* at 2°C as described by Tollervey (48) for yeast spheroplast RNAs. RNA was recovered from gradient fractions by hot phenol extraction as described below. To examine the effects of heat treatment on RNA distribution in sucrose gradients, lysate aliquots were incubated at 42 or 65°C for 3 min and then chilled 5 min on ice before separation on sucrose gradients.

Examination of RNAs and proteins. For RNA isolation, cellular fractions or immunoprecipitates were adjusted to 0.5% SDS and 0.1 U of proteinase K per ml and incubated at 65°C for 15 min. RNA was extracted from samples once with phenol at 65°C and twice with phenol-chloroform-isoamyl alcohol (50:48:2) and then precipitated with ethanol.

For Northern (RNA) analysis, small RNAs were electrophoresed on 6% polyacrylamide–8 M urea gels and electroblotted to Nytran membranes; large RNAs were separated on 1% formaldehyde gels and capillary transferred to Nytran membranes. Membranes were hybridized to various probes in 5× SSPE (1× SSPE is 0.18 M NaCl, 10 mM $NaPO_4$, and 1 mM EDTA [pH 7.7])–5× Denhardt's solution–0.1% SDS–50 mg of *E. coli* tRNA per ml. Probes used included an Sp6-promoted transcript complementary to RNA B produced from plasmid pGB.2, which contains the *T. brucei* *Fok*I-*Bam*HI RNA B gene fragment cloned into *Eco*RI-*Bam*HI-digested pGEM-3Z (56). Oligonucleotide probes complementary to the indicated residues of small RNAs were SL (106 to 125), U2 (1 to 20), U4 (90 to 109), U6 (1 to 16), RNA B (1 to 25), $tRNA^{Leu}$ (35 to 56), and 5.8S (1 to 25). DNA probes complementary to the 5' ETS, ITS1, and ITS2 regions of *T. brucei* were amplified DNAs made via the polymerase chain reaction, using a cloned *T. brucei* rRNA repeat, pR4 (57), as the template. The 342-bp ITS1 and 590-bp ITS2 DNAs were made by using primers corresponding to the 5' and 3' ends of the regions; the 1.3-kb ETS DNA was made with primers corresponding to a site 260 nt 5' of the transcription start and to the 5' end of 18S rRNA. Sequences of the oligonucleotide primers were as follows:

rITS1-5', GGAATTCTGATATCCATTATACAAAAAAGAGC
cITS1-3', AAAGCTTGTGGGAGCCGTGGTCAACAGGGAGA
rITS2-5', GGAATTCATATAAAAACAAAACACACACCTATTTT
cITS2-3', AAAGCTTAAAATGCAATATAAAAAAGTGAAGCGTA
rpETS-5', GCTCTAGACTTTCCACCCAGCGCGGG
c18S-5', ATAAGCTTCTGGCAGAATCAACCAGATC

Precursor rRNA was detected by primer extension with avian myeloblastosis virus reverse transcriptase (Promega), using the manufacturer's recommended conditions. The oligonucleotide primer, crRNA, was radiolabelled at the 5' end with T4 polynucleotide kinase and [γ-^{32}P]ATP. crRNA contains the sequence CTGTGAAGGTAATTAAAAACC, which is complementary to residues within the ETS region of the pre-rRNA, located 240 to 260 nt downstream of the transcription start site and 126 to 146 nt downstream of the primary processing site (57). Primer extension products were separated by electrophoresis through 6% polyacrylamide–8

M urea gels; the product corresponding to the pre-rRNA primary processing site, which was 50- to 100-fold more abundant than the product corresponding to the transcription start site, is shown in Fig. 3.

For analysis of RNAs present in immunoprecipitates, RNAs were radiolabelled at their 3′ ends with [5′-^{32}P]pCp (3,000 Ci/mmol; NEN) and T4 RNA ligase. End-labelled RNAs were fractionated on 6% polyacrylamide–8 M urea gels of 0.3-mm thickness, which were dried onto paper for autoradiography.

Samples for Western immunoblot analysis were prepared by sonication of whole cells or immunoprecipitates in loading buffer (2% SDS, 100 mM DTT, 60 mM Tris-HCl [pH 6.8], 0.01% bromphenol blue). Material from approximately 10^7 cells, or the immunoprecipitate from 10^8 cells, was loaded per lane. Samples were electrophoresed through a 5% stacking gel into an SDS-polyacrylamide gel (12% polyacrylamide) and then transferred electrophoretically to a nitrocellulose membrane. The membrane was incubated with anti-*Physarum* fibrillarin ascites fluid antibody (1:5,000 dilution) and then either incubated with an anti-mouse IgG alkaline phosphatase conjugate (Promega) and stained with the chromogenic substrates bromochloroindolyl phosphate and nitroblue tetrazolium or incubated with an anti-mouse IgG horseradish peroxidase-linked whole antibody and visualized with enhanced chemiluminescence Western blotting detection reagents (Amersham).

Oligonucleotide-directed RNase H digestion of snRNAs. [5′-^{32}P]pCp-labelled RNAs isolated from immunoprecipitates were suspended in 20 mM HEPES-KOH (pH 7.9)–50 mM KCl–10 mM $MgCl_2$–1 mM DTT–1 μg of 16S and 23S *E. coli* rRNAs per ml–4 mM specified oligonucleotide, heated to 95°C for 3 min, and then slowly cooled to 37°C; 0.8 U of Promega RNase H was added, and digestion proceeded for 40 min before the reaction was stopped with 50 mM EDTA. Samples were adjusted to 50% formamide, denatured at 95°C, and separated electrophoretically on a 0.3-mm-thick 6% polyacrylamide–8 M urea gel, which was dried before autoradiography.

RESULTS

Structural similarity between RNA B and U3 snRNAs. U3 snRNA sequences from a number of organisms of diverse phyla have been characterized (12); they are approximately 215 nt in size, the exceptions being the U3 snRNAs of *Schizosaccharomyces pombe* (256 nt) and of *Saccharomyces cerevisiae* (328 nt). The U3 snRNAs are not well conserved in primary sequence; they share only four small regions of strong homology (boxes A to D) (20, 23, 35). Primary sequence similarities detected between the 144-nt RNA B of *T. brucei* (31) and U3 snRNAs are shown in Fig. 1A. The 5′ 33 residues of RNA B and mammalian U3 snRNAs share 70% identity. The box A homology, which is the most highly conserved region of U3 snRNAs, is found within this 5′ region of RNA B; 12 of 15 residues can be aligned between RNA B and box A by allowing a one-nucleotide shift within each sequence. Two candidates for a box C homology are identified in RNA B. The box C sequence is protected by proteins in the U3 snRNP (34) and is found in several nucleolar snRNAs which associate with the nucleolar protein, fibrillarin (3, 55). Unequivocal sequence homologies between the box B and box D regions of U3 snRNAs were not identified in RNA B.

A phylogenetically determined secondary structure for U3 snRNAs has been proposed and supported by RNase digestion and chemical modification studies of HeLa and *Xenopus* U3 snRNAs (23, 34). However, it is recognized that the 5′ regions of U3 snRNAs of unicellular organisms and plants do not conform to this model (26, 35), although all U3 snRNAs seem to retain structural similarity in their 3′ domains. The small size and diverse sequence of RNA B relative to U3 snRNA sequences made complete sequence alignments unfeasible; however, a secondary structure model for RNA B was suggested by comparison of RNA B sequences from distantly related trypanosomatids (Fig. 1B) (15). The 5′ end of RNA B could form a stem-loop structure containing the box A homology, which is comparable to the first stem-loop structure proposed for nonvertebrate U3 snRNAs (26, 35). The 3′ structure of RNA B differs significantly from models proposed for other U3 snRNAs, largely because of the small size of RNA B; common features include a possible central stem structure and positioning of the box C-like sequences within single-stranded regions consistent with roles in protein binding. The validity of the RNA B secondary structure model remains to be tested by chemical and enzymatic methods.

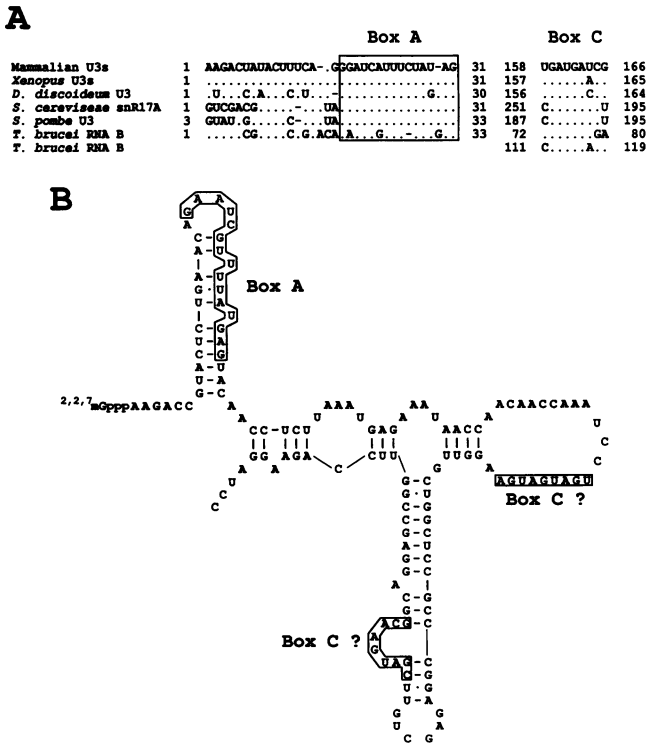

FIG. 1. (A) Box A and box C homologies of U3 snRNAs compared with *T. brucei* RNA B sequences. U3 sequences are taken from references 20, 23, and 35. (B) Putative secondary structure of *T. brucei* RNA B. Box A and potential box C homologies are boxed.

A 35-kDa *T. brucei* protein shares epitopes with fibrillarin. Fibrillarin is a ubiquitous and highly conserved nucleolar protein which ranges in apparent molecular mass between 34 and 36 kDa among species (2, 8, 13, 21, 28). Western analysis of proteins from *T. brucei* whole cell extracts separated by SDS-polyacrylamide gel electrophoresis was performed, using a monoclonal antibody (P2G3) raised against *Physarum* fibrillarin (8) (Fig. 2). Antibody P2G3 recognizes a common epitope on fibrillarin proteins of diverse species (8, 13). A major polypeptide of approximately 35 kDa was detected by

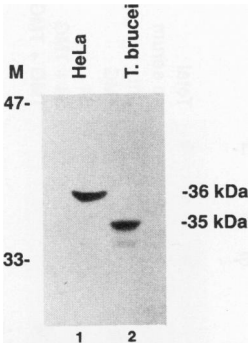

FIG. 2. Identification of the *T. brucei* fibrillarin protein. Whole cell extracts of HeLa (lane 1) and *T. brucei* (lane 2) cells were electrophoresed through a 12% polyacrylamide gel. Proteins immobilized on a nitrocellulose membrane were detected with anti-*Physarum* fibrillarin antibody P2G3 plus anti-mouse alkaline phosphatase-conjugated antibodies and enzymatic staining. Locations (kilodatrons) of prestained Bio-Rad protein markers are shown on the left.

this antibody in *T. brucei* extracts; similar-size polypeptides were also detected in *Crithidia fasciculata* and *Leptomonas collosoma* (data not shown). A polypeptide of 34 kDa was also detected, but this polypeptide appears to be a degradation product of fibrillarin, as it was present in higher abundance when protease inhibitors were omitted from extract preparations (data not shown). The HeLa fibrillarin migrates at 36 kDa in this gel system, although its gene sequence predicts a polypeptide of 34 kDa (2, 21). It has been reported that a human scleroderma serum identifies nucleolar structures in *T. brucei* (43), likely as a result of autoantibody recognition of conserved fibrillarin epitopes present in the polypeptides detected in this assay.

RNA B and fibrillarin are localized in nucleolar fractions. The association between nucleolar snRNAs and nucleoli has been classically established by cellular fractionation methods designed to purify dense, nucleolar structures (38, 55) as well as by microscopic methods (37). Nucleoplasmic snRNAs are typically extracted from nuclear fractions more readily than are the nucleolar snRNAs (48, 55, 58). Preliminary experiments indicated that RNA B was more difficult to solubilize than were the known nucleoplasmic snRNAs in both whole cell and nuclear extracts (56). Using the nucleolar components, fibrillarin and pre-rRNAs, and the nucleoplasmic snRNAs as markers, it was possible to determine the nuclear compartment occupied by RNA B.

T. brucei cells were separated into cytoplasmic, nuclear, nucleoplasmic, and nucleolar fractions. Nuclei prepared from *T. brucei* cells broken by Dounce homogenization were disrupted by sonication, and nucleoplasmic and nucleolar fractions were separated on a sucrose step gradient (see Materials and Methods). Figure 3 shows the distribution of various small RNAs as well as fibrillarin protein and pre-rRNA in these fractions. Purified nuclei were free of soluble cytoplasmic material, as demonstrated by the absence of $tRNA^{Leu}$ in nuclear fractions. The majority of each U RNA species was retained in the nuclear fraction, though moderate amounts of SL RNA were found in the cytoplasmic fraction; significant proportions of SL RNA are commonly lost to the cytoplasm during nuclear isolation (56; data not shown). For each of the nucleoplasmic snRNAs (SL, U2, U4, and U6), the amount retained in the nuclear fraction was fully recovered in the nucleoplasmic fraction. In contrast,

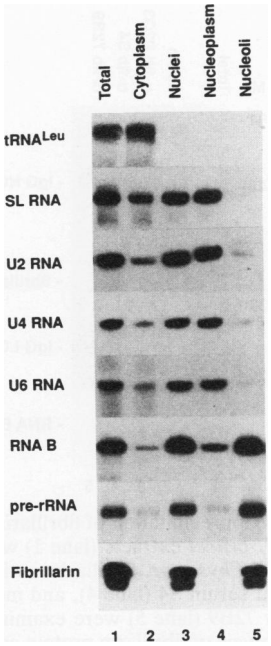

FIG. 3. Distribution of small RNAs and fibrillarin in subcellular fractions. *T. brucei* cells were fractionated as described in the text. Lanes contain cellular equivalents of total (lane 1), cytoplasmic (lane 2), nuclear (lane 3), nucleoplasmic (lane 4), and nucleolar (lane 5) fractions. The top six panels show Northern analysis of RNAs extracted from subcellular fractions; oligonucleotides complementary to the indicated RNAs were used as probes. The seventh panel shows a primer extension product corresponding to a region within the 5′ ETS region of the pre-rRNA (see Materials and Methods). The bottom panel shows Western analysis of fibrillarin protein, using chemiluminescence detection as described in Materials and Methods.

RNA B segregated with the dense nucleolar fraction. The fractionation properties of fibrillarin and pre-rRNAs closely resemble those of RNA B in this experiment; each is found predominantly in the nuclear versus the cytoplasmic fraction, and each is pelleted through the sucrose step gradient following sonication of nuclei, confirming that nucleolar material is indeed represented in this fraction. Thus, RNA B fractionates distinctly from cytoplasmic and nucleoplasmic snRNAs and fractionates in parallel with components of the nucleolus.

Coimmunoprecipitation of *T. brucei* fibrillarin and RNA B. The possibility that RNA B is closely associated with fibrillarin, perhaps in an snRNP-like particle, was examined by immunoprecipitation of fibrillarin and associated RNAs from *T. brucei* whole cell extracts. Several antibodies were tested for the ability to immunoprecipitate *T. brucei* fibrillarin protein, as assessed by Western analysis; the presence of RNA B in immunoprecipitates was evaluated by Northern analysis (Fig. 4). The monoclonal anti-*Physarum* fibrillarin antibody P2G3 was unable to immunoprecipitate fibrillarin or RNA B (Fig. 4, lane 3), though it does react with *T. brucei* fibrillarin by Western analysis, suggesting that the epitope recognized may be available only on denatured *T. brucei* fibrillarin. Similarly, precipitation of fibrillarin-associated RNAs from *Physarum* extracts with antibody P2G3 has not been demonstrated (7). The monoclonal anti-mouse U3 RNP antibody 72B9 (39), which has been used successfully to immunoprecipitate fibrillarin and associated U3, U8, and

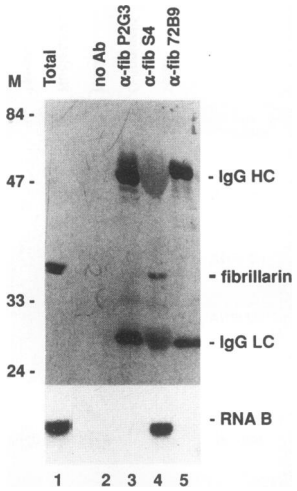

FIG. 4. Coimmunoprecipitation of fibrillarin and RNA B. Immunoprecipitates of *T. brucei* extracts (lane 1) with no antibody (lane 2), monoclonal anti-*Physarum* fibrillarin antibody P2G3 (lane 3), scleroderma patient serum S4 (lane 4), and monoclonal anti-mouse (U3)RNP antibody 72B9 (lane 5) were examined. The upper panel shows Western analysis of fibrillarin protein as described for Fig. 2; IgG heavy chains (HC) and light chains (LC) are visible in each immunoprecipitate as a result of reaction with the anti-mouse alkaline phosphatase-conjugated antibody. Positions (kilodaltons) of prestained Bio-Rad protein markers are shown on the left. The lower panel shows Northern analysis of RNA B present in RNAs extracted from immunoprecipitates.

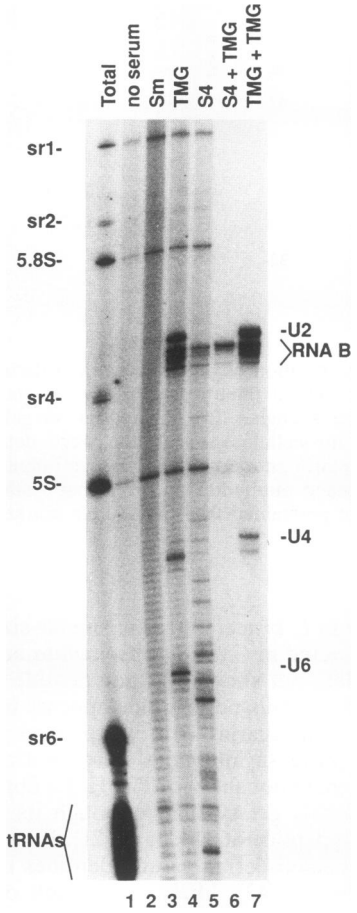

FIG. 5. Identification of small RNAs associated with fibrillarin by immunoprecipitation. Immunoprecipitated RNAs were radiolabelled at their 3′ ends and fractionated on a 0.3-mm 6% polyacrylamide–8 M urea gel. Lane 1 shows total RNA from 1/100 the amount of cells used in other lanes. Lanes 2 to 5 show RNAs immunoprecipitated directly from whole cell extracts with no serum (lane 2), anti-Sm serum (lane 3), anti-TMG cap antibody (lane 4), and scleroderma patient serum S4 (lane 5). Samples in lanes 6 and 7 are reprecipitations with anti-TMG cap antibodies of heat-treated RNAs purified from the samples in lanes 5 and 4, respectively. Positions of the small 28S rRNAs (sr1 [214 nt], sr2 [183 nt], sr4 [135 nt], and sr6 [76 nt]), the 5.8S (169 nt) and 5S (119 nt) rRNAs, the tRNAs, and the abundant U snRNAs (U2 [147 nt], RNA B [140 to 144 nt], U4 [106 nt], and U6 [91 nt]) are indicated.

U13 snRNAs from HeLa cells (55) and U3 snRNA from yeast cells (18), also did not immunoprecipitate *T. brucei* fibrillarin or RNA B (lane 5). However, autoimmune antibodies in scleroderma patient serum S4, which are monospecific for human fibrillarin (40) and which react with fibrillarin from diverse organisms (21, 28, 40, 42), immunoprecipitated fibrillarin and associated RNA B from *T. brucei* cell extracts (lane 4); the antibodies did not react with RNA B alone (data not shown).

The coimmunoprecipitation of RNA B and fibrillarin by serum S4 indicates that the molecules are closely associated, perhaps in an snRNP-like particle or complex. Approximately 10% of both the fibrillarin and RNA B present in extracts was immunoprecipitable. Similarly, only 10 to 20% of HeLa U3 snRNA is precipitable by various antifibrillarin antibodies (33). Immunoprecipitation of RNA B was optimal from extracts prepared with 200 mM NaCl; increasing the salt concentration to 300 mM allowed for better extraction of RNA B but decreased RNA B immunoprecipitation with serum S4 (data not shown). Comparably, the efficiency of HeLa U3 and U13 snRNP precipitation with antifibrillarin antibodies diminished when extracts were prepared with salt concentrations above 200 mM, consistent with dissociation of fibrillarin antigen from these snRNAs at higher salt concentrations (34, 55). These observations suggest that fibrillarin association with nucleolar snRNAs is somewhat loose or indirect, in contrast to the salt-stable interactions observed between protein and RNA components of nucleoplasmic snRNPs (5).

To determine whether other species of snRNAs are associated with fibrillarin in *T. brucei*, small RNAs immunoprecipitated from whole cell extracts with antifibrillarin and anti-TMG cap antibodies were examined by radiolabelling at their 3′ ends with [^{32}P]pCp and separation on denaturing polyacrylamide gels (Fig. 5, lanes 2 to 5). Anti-Sm serum, which does not precipitate *T. brucei* U snRNPs, was included as a control. Background levels of the small rRNAs are present in control and experimental lanes. The pattern of major *T. brucei* snRNA species precipitable by anti-TMG cap antibodies is seen in lane 4; U2 (147 nt), RNA B (140 to 144 nt), U4 (106 nt), and U6 (91 nt) snRNAs are detected. The multiple species attributed in this study to RNA B (see below) have not been previously described; they are likely due to heterogeneity at the 3′ end and may be strain specific. Scleroderma patient serum S4 precipitated the RNA B species as well as several minor species, migrating at 129, 111, 108, 106, 102, 99, 96, 94, 93, 92, 90, 88, and 73 nt (lane 5). This pattern of minor species was reproducible, although variations in the relative abundance of each species were sometimes noted. None of these bands could be attributed to

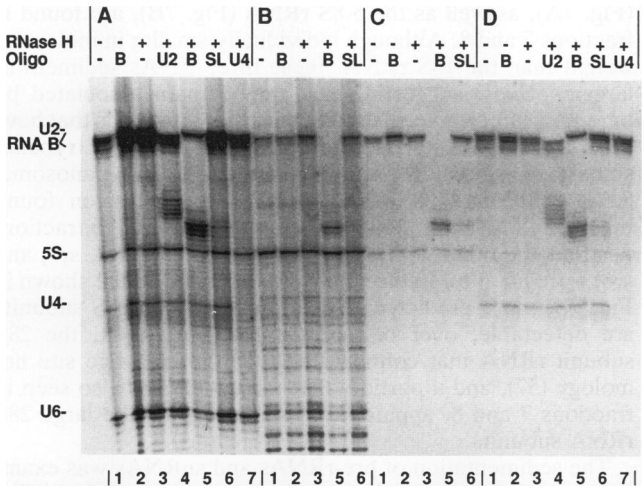

FIG. 6. Identification of immunoprecipitated RNAs by oligonucleotide-directed RNase H digestion. Aliquots of the RNA samples shown in lanes 4 to 7 of Fig. 5 are analyzed in panels A to D, respectively. RNAs precipitated from whole cell extracts with anti-TMG cap antibody (A) and with scleroderma patient serum S4 (B) and RNAs from serum S4 (C) and anti-TMG cap antibody (D) precipitates reprecipitated with anti-TMG cap antibody were 3′ end labelled. Samples were then hybridized to oligonucleotides complementary to snRNAs, incubated with RNase H to degrade RNA-DNA complexes, and separated on a denaturing 6% polyacrylamide gel. Samples in lanes 1 were mock treated. Oligonucleotides complementary to RNA B (lanes 2 and 5), to U2 snRNA (lanes 4), to SL RNA (lanes 6), and to U4 snRNA (lanes 7) were present in the indicated samples; RNase H was present in samples shown in lanes 3 to 7. Positions of the U2, RNA B, U4, and U6 snRNAs and of the 5S rRNA are indicated.

RNA B degradation, as assessed by Northern analysis using an anti-RNA B transcript as a probe (data not shown). To test whether some of these RNAs might represent pre-rRNAs or rRNAs, Northern blots were also probed with ETS, ITS1, and ITS2 DNAs as well as rRNA repeat unit DNA; no hybridization with any of these sequences was detected (data not shown). Direct analysis of these fibrillarin-associated RNAs will be required to ascertain their identities. The observation that RNase-protected fragments of synthetic rRNAs containing the 28S α-sarcin site were precipitated from HeLa cell extracts with antifibrillarin antibodies led to the suggestion that U3 snRNA might interact with 28S rRNA in vivo (34). However, we observe that the 182-nt 28S rRNA, sr2, which contains the α-sarcin cleavage site (57), was not precipitated from *T. brucei* whole cell extracts with scleroderma patient serum S4.

To establish which of the fibrillarin-associated RNAs in *T. brucei* have TMG cap structures, the RNAs were purified and immunoprecipitated with the monoclonal anti-TMG antibody prior to radiolabelling. Lane 6 in Fig. 5 shows that only the 140- to 144-nt RNA B species were specifically immunoprecipitated (see below); overexposures of the gel did not reveal other species, although species up to 100-fold less in concentration than RNA B should have been detected in these experiments. An RNA of 120 nt seen in lanes 6 and 7 (and control lanes not shown) corresponds to the *E. coli* 5S RNA, present in the carrier RNA used in immunoprecipitation reactions. Heat treatment of RNAs before immunoprecipitation effectively dissociated hydrogen-bonded RNAs, as judged by the absence of the U6 snRNA in lane 7; the γ-monomethyl phosphate-capped U6 is normally hydrogen bonded with U4 snRNA and thus precipitated from extracts (as in lane 3). No specific RNA interactions were disrupted by the heat treatment of RNAs present in scleroderma patient serum S4 immunoprecipitates (data not shown); thus, RNA B apparently does not hydrogen bond with any of the small RNAs identified in lane 5.

The identities of the TMG-capped RNAs immunoprecipitated by scleroderma patient serum S4 and anti-TMG antibody were established by oligonucleotide-directed RNase H digestion (Fig. 6) and by Northern analysis (data not shown). Aliquots of RNAs from the experiment shown in Fig. 5 were radiolabelled at their 3′ ends, incubated with an oligonucleotide complementary to U2, RNA B, U4, or SL RNA, and then digested with RNase H, which specifically degrades RNA duplexed with DNA. The RNAs shown in lanes 4 to 7 of Fig. 5 are thus analyzed in experiments shown in Fig. 6A to D, respectively. RNase H specifically degrades the 147-nt band in the presence of an oligonucleotide complementary to residues 1 to 20 of U2 snRNA and degrades the 106-nt band in the presence of an oligonucleotide complementary to residues 90 to 109 of U4 snRNA (Fig. 6). All of the RNAs with sizes of 140 to 144 nt, found in scleroderma patient serum S4 and anti-TMG antibody immunoprecipitates, are degraded by RNase H in the presence of an oligonucleotide complementary to RNA B (residues 1 to 25) (Fig. 6). The 140-nt species is labelled less intensively in this experiment than in that shown in Fig. 5, although the same RNA sample was used for each labelling, suggesting that the RNA B pattern can be altered artifactually during 3′ end labelling with [5′-^{32}P]pCp. Because the RNAs under investigation were similar in size to SL RNA (139 nt), an oligonucleotide complementary to residues 5 to 24 of SL RNA was included as a control in this experiment. Minor degradation occurred in each RNA sample following RNase H digestion; however, this degradation is likely due to small sequence complementarity (9 of 12 residues) between RNA B (residues 15 to 26) and the anti-SL oligonucleotide (residues 5 to 16) rather than the presence of SL RNAs in immunoprecipitates; no SL RNA was detected by Northern analysis (data not shown). This experiment shows that RNA B is the only TMG-capped RNA immunoprecipitated by scleroderma patient serum S4, since all detectable RNAs were digested by RNase H in the presence of an oligonucleotide complementary to RNA B, and no underlying RNAs were revealed by this procedure.

Cosedimentation of RNA B and pre-rRNAs in nondenaturing sucrose gradients. The coincident immunoprecipitation and subcellular fractionation of RNA B and fibrillarin protein identified RNA B as a nucleolar snRNA. The ability of RNA B to associate with pre-rRNAs was next evaluated, since U3 and other nucleolar snRNAs appear to interact with pre-rRNAs through hydrogen bonding (11, 36, 48, 58). The yeast nucleolar snRNAs are associated with pre-rRNAs following fractionation of gently deproteinized RNAs on sucrose gradients (48, 58). Similar analysis of *T. brucei* RNAs was performed; *T. brucei* lysates were deproteinized with proteinase K in the presence of 2% SDS at 14°C, and then cleared lysates were centrifuged through a 10 to 30% nondenaturing sucrose gradient. The profiles of large RNAs and small RNAs isolated from gradient fractions are shown in Fig. 7A and B, respectively. The distribution of RNA species is consistent with separation of protein-free RNAs under conditions in which RNA-RNA interactions have been maintained. The mature 2.3-kb 18S rRNA is found primarily in fractions 5 and 6, with smaller amounts seen in fractions 7 and 8, whereas the 1.8-kb 28Sα and the 1.6-kb 28Sβ rRNAs

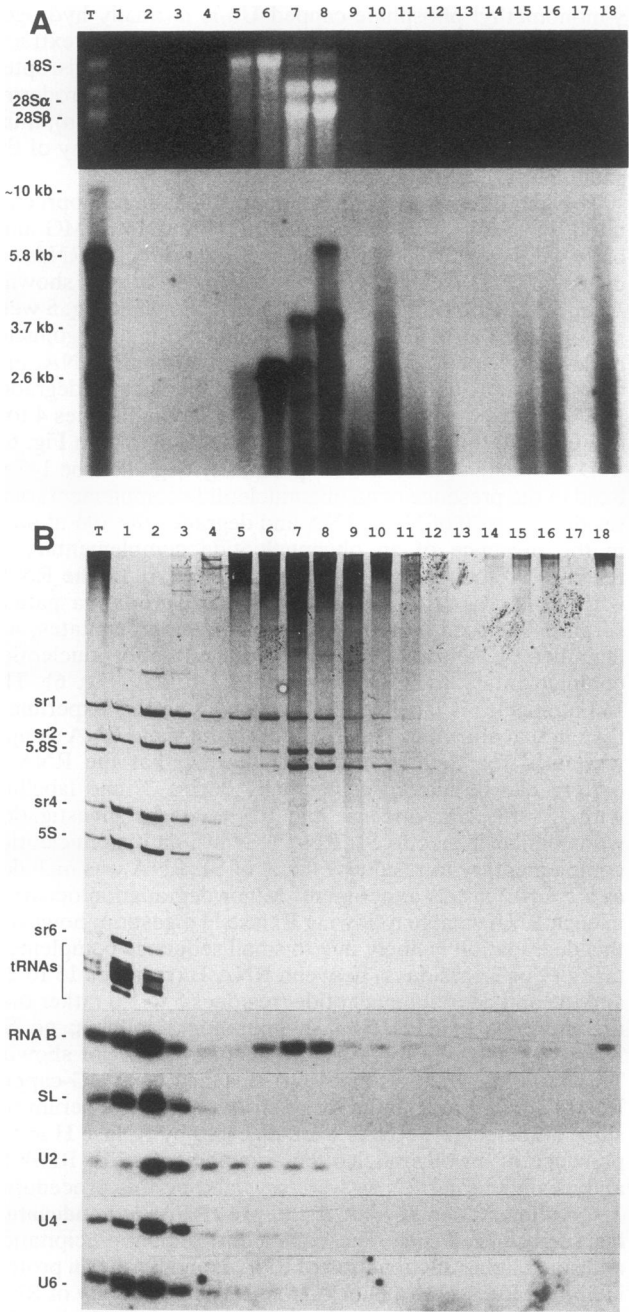

FIG. 7. Distribution of deproteinized RNAs on a nondenaturing sucrose gradient. Total RNA was deproteinized under nondenaturing conditions and centrifuged through a 10 to 30% sucrose gradient as described by Tollervey (48). RNAs were isolated from fractions under denaturing conditions. Fraction 1 is from the top of the gradient, and fraction 18 is from the bottom; lane T contains total RNA isolated from the initial extract. (A) Profile of high-molecular-weight RNAs separated on a 1% formaldehyde gel. The pattern of mature RNAs is visualized by ethidium bromide staining of the gel in the top panel. The lower panel shows the distribution of precursor rRNAs (see Fig. 8) detected by hybridization of ETS, ITS1, and ITS2 DNAs to a Northern transfer of the gel. (B) Profile of low-molecular-weight RNAs separated on a 6% polyacrylamide–8 M urea gel. In the top panel, a silver-stained gel shows the pattern of 28S rRNAs (sr1, sr2, sr4, and sr6), 5.8S and 5S rRNAs, and tRNAs. Lower panels are Northern blots of duplicate gels hybridized with oligonucleotides complementary to the indicated RNAs.

(Fig. 7A), as well as the 5.8S rRNA (Fig. 7B), are found in fractions 7 and 8. Although individually smaller in molecular weight than the 18S rRNA, these three RNAs sediment as larger species, suggesting that they remain associated by long-range intermolecular base-pairing interactions that have been predicted by secondary structure modeling of trypanosomal large-subunit (LSU) rRNAs (6, 16, 46). Trypanosomal 5.8S, 28Sα, and 28Sβ subunit rRNAs have been found together following low-temperature phenol extraction, whereas the other 28S subunit fragments (sr1, sr2, sr4, and sr6) were not (46). In the sedimentation experiment shown in Fig. 7B, more predicted interactions between 28S subunits are detectable; over half of the total sr2 RNA, the 28S subunit rRNA that contains the α-sarcin cleavage site homology (57), and a portion of the sr1 RNA are also seen in fractions 7 and 8, apparently associated with the large 28S rRNA subunits.

The sedimentation of pre-rRNAs and snRNAs was examined to look for potential hydrogen-bonded associations. The profile of pre-rRNAs was illuminated by hybridization of a Northern blot of this gel with 5′ ETS, ITS1, and ITS2 DNAs both collectively (Fig. 7A) and individually (data not shown). The putative primary precursor of approximately 10 kb which is detected in the total RNA lane (Fig. 7A, lane T) does not appear in gradient fractions; it presumably is processed or degraded too quickly for examination by this analysis. Three major intermediates of *T. brucei* rRNA processing (Fig. 8) are identified in the control lane. Of these, the 3.7-kb pre-rRNA containing the 5′ ETS, 18S rRNA, and ITS1 is found in fractions 7 and 8, with minor amounts in fraction 6. A 2.6-kb pre-rRNA containing 18S rRNA and ITS1 is predominant in fraction 6, with large amounts also in fractions 7 and 8. The 5.8-kb pre-RNA containing the 5.8S, ITS2, and 28S rRNA sequences is found in fraction 8. A previously identified 5.0-kb pre-RNA containing the 28S sequences (57) was detected in fraction 8 when probed with a cloned rDNA repeat (data not shown). The profiles of small RNAs are shown in Fig. 7B. The known nucleoplasmic snRNAs, SL, U2, U4, and U6 snRNAs, are found primarily in the first few fractions (detected by Northern analysis) along with other free, small RNAs such as the tRNAs and 5S rRNA (detected by silver staining). In contrast, one peak of RNA B is found in the first three fractions of the gradient, whereas a second strong peak of RNA B is found in fractions 6, 7, and 8 primarily where the 3.7- and 2.6-kb pre-18S rRNAs are located; in addition, 28S and 5.8S rRNA precursors are found in fraction 8. Association of RNA B with intermediates of 18S rRNA suggests a role for RNA B in 18S maturation. Whether RNA B is associated with 28S rRNA precursors cannot be determined by this analysis, since the distribution of pre-28S rRNAs overlaps that of the 18S precursors.

RNA B cosedimention with pre-rRNAs on nondenaturing sucrose gradients in the absence of proteins suggests that RNA B is associated with pre-rRNAs by hydrogen bonding. Support for this hypothesis is demonstrated in Fig. 9, which shows the gradient profiles of RNA B and 5.8S rRNA present in deproteinized cell extracts that were briefly heat treated before fractionation. The putative interactions between RNA B and pre-rRNAs are disrupted at 42°C, as evidenced by the loss of RNA B migration with higher-molecular-weight RNAs; RNA B is found only at the top of the gradient where free small RNAs are fractionated. 5.8S rRNA, which is predicted to form multiple intermolecular helices with 28Sα rRNA (6, 14, 46), remains associated with higher-molecular-weight RNAs at 42°C; partial disruption of

these interactions occurs by heat treatment of RNAs at 65°C, as indicated by loss of the distinct 5.8S peak corresponding to comigration with 28S rRNAs and by the appearance of significant amounts of 5.8S at the top of the gradient. The apparent release of RNA B and 5.8S RNAs from interactions with high-molecular-weight RNAs following heat treatment is consistent with disruption of hydrogen-bonded associations. The putative interactions between RNA B and pre-rRNAs are more labile than interactions between 5.8S rRNA and 28S rRNAs.

DISCUSSION

This work shows that RNA B, an abundant, TMG-capped U snRNA of trypanosomatids, shares structural features and fractionation properties with U3 and other nucleolar snRNAs. RNA B is located in nucleoli, as judged from its coincident subfractionation with the nucleolar protein, fibrillarin, and precursor rRNAs. It is the only TMG-capped U snRNA of *T. brucei* found in association with fibrillarin by coprecipitation with antifibrillarin antibodies. RNA B appears hydrogen bonded to pre-rRNAs, as evaluated by sedimentation of deproteinized RNAs through sucrose gradients, suggesting that RNA B functions in rRNA processing. From these data, we conclude that RNA B represents a diverged form of the U3 snRNA, ubiquitous to all other organisms examined in animal, plant, and protist kingdoms (12).

The initial characterization of RNA B indicated partial sequence homology with U3 snRNAs, although not enough to propose an identity with U3 or other known RNAs (31). Extensive regions of sequence complementarity noted between RNA B and SL RNA or U2 snRNA of *T. brucei* also suggested a potential role in *trans* splicing. Completion of a phylogenetic analysis revealed that these complementarities were not upheld between snRNAs from different trypanosome species, whereas putative nucleolar snRNP protein

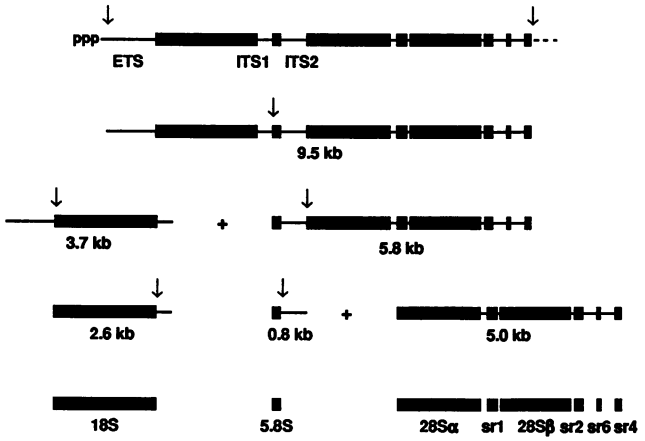

FIG. 8. Deduced pathway of *T. brucei* pre-rRNA processing. Stable RNA intermediates identified by Northern hybridization analysis with rDNAs (57) or transcribed spacer DNAs (this work) are shown; arrows indicate cleavage sites. ETS, ITS1, and ITS2 sequences hybridize to the putative primary precursor of approximately 10 kb. ETS DNA hybridizes to the 3.7-kb 18S precursor, and ITS1 DNA hybridizes to the 3.7- and 2.6-kb 18S precursors. ITS2 DNA hybridizes to the 5.8-kb precursor of 5.8S and 28S rRNAs and to the 0.8-kb 5.8S precursor (data not shown). The 5.0-kb species is not detected with ETS, ITS1, or ITS2 DNA but is detected with rDNA sequences (data not shown).

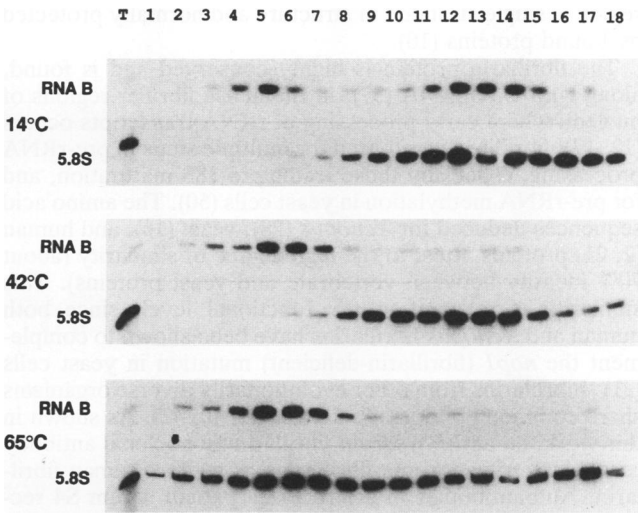

FIG. 9. Distribution of RNA B and 5.8S rRNA on nondenaturing sucrose gradients following heat treatment. Deproteinized total RNA was prepared at 14°C as for Fig. 7. Aliquots were either untreated (top panel) or briefly treated at 42°C (middle panel) or at 65°C (bottom panel) before separation on 5 to 20% sucrose gradients. RNAs isolated from gradient fractions 1 to 18 (top to bottom) were analyzed by Northern analysis for RNA B and 5.8S rRNA as indicated; lane T contains total, unfractionated RNA. The patterns of RNA distribution are shifted from those shown in Fig. 7 as a result of differences in sucrose gradient densities, as indicated.

binding regions, the box C homologies, were conserved (15). In addition, a reasonable match to the box A region of U3 snRNAs is conserved in RNA B, but sequences with strong similarity to the box B or box D consensus sequences are not found. Because these regions are conserved between other U3 snRNAs and are thus likely to represent functionally important sequences, it is possible that functionally equivalent sequences occur in RNA B but are too divergent to recognize. Alternatively, these sequences may be unnecessary for U3-like functions in trypanosomes.

The box C homology, conserved in all U3 snRNAs and in RNA B, is present in several other nucleolar RNAs, including the HeLa U8, U13, X, and Y snRNAs (55), the yeast U14 (snr128) and snr190 snRNAs (58), and the mouse U14 snRNA (4.5S hybRNA) (51). Each of these snRNAs except RNA B also contains a less highly conserved box D homology (PuUCUGA). Initially, immunoprecipitation of these nucleolar snRNAs from cell extracts by antifibrillarin antibodies, particularly of RNase A- or T_1-protected fragments of HeLa U3 containing boxes C and D (34), suggested that fibrillarin associates with nucleolar snRNAs via these conserved regions. Mutations in the box C and D regions of the essential U14 snRNA of yeast cells prevented U14 snRNA accumulation; the cold sensitivity of mutants suggested that protein-RNA interactions might be affected (22). Recently, mutational analysis of in vitro-synthesized human U3 snRNAs determined that the box C sequence is required for reconstitution with fibrillarin in whole cell extracts, whereas the box D sequence is not (3). This finding is consistent with the presence of box C and absence of box D homologies in RNA B, which is immunoprecipitable by antifibrillarin antibodies. The box C domain found at residues 72 to 80 in RNA B is accessible to binding by oligonucleotides in naked RNA B in vitro but not to RNA B in vivo, suggesting that this

region is single stranded in structure and normally protected by bound proteins (10).

The fibrillarin protein is highly conserved and is found, along with U3 snRNA (37), in the dense fibrillar regions of nucleoli where early processing of rRNA transcripts occurs (12, 17); fibrillarin is required for multiple steps in pre-rRNA processing, especially those leading to 18S maturation, and for pre-rRNA methylation in yeast cells (50). The amino acid sequences deduced for *Xenopus* (28), yeast (16), and human (2, 21) proteins attest to the high degree of similarity (about 70% identity between vertebrate and yeast proteins). This similarity is relevant at the functional level, since both human and *Xenopus* fibrillarins have been shown to complement the *nop1* (fibrillarin-deficient) mutation in yeast cells (21). Fibrillarins from other evolutionarily diverse organisms share common epitopes (8, 21, 28, 39, 40, 42). As shown in this work, an anti-*Physarum* fibrillarin monoclonal antibody recognizes trypanosome fibrillarins as well as human fibrillarin. Autoantibodies in scleroderma patient serum S4 recognizes *T. brucei* fibrillarin; a related serum has detected nucleolar structures in *T. brucei* (43). However, the epitope recognized by monoclonal antibody 72B9 in mammalian and yeast fibrillarins is absent from the *T. brucei* fibrillarin. It is interesting that fibrillarin, a nucleolar snRNP-associated protein, and the box C sequence, a putative binding domain for common nucleolar snRNPs, are conserved in the evolutionarily ancient trypanosomatids. In contrast, the nucleoplasmic snRNAs of *T. brucei* do not contain the Sm antigen binding site, and their snRNPs do not share Sm antigen epitopes, elements which have been conserved in all other eukaryotes examined.

The 5′ region of U3 snRNAs including the box A homology is of particular interest because evidence indicates it may be a functional domain; its conservation in RNA B implies comparable function. Cleavage of the primary processing site of the 5′ ETS region, which appears to be a conserved event commencing pre-rRNA processing (12), has been demonstrated in vitro in mouse cell extracts (24); oligonucleotide-directed destruction of the 5′ region of U3 snRNA, containing box A, abolished ETS cleavage (25). Psoralen cross-links generated between mammalian and yeast U3 snRNAs and 5′ ETS rRNAs have been mapped within or adjacent to the box A homology, demonstrating close proximity of these sequences, likely during processing (4, 30, 47). In rat, cross-links were formed in a region of the ETS containing sequences required for primary cleavage, as identified in mouse extracts (9); 11 residues within this region and 3′ adjacent to the processed site are conserved between mammals and frogs, whereas only limited amounts of identity have been noted between related cleavage sites in more phylogenetically diverse organisms (4, 19). In yeast cells, two distinct sites of U3 snRNA interaction with the ETS were precisely mapped. The upstream site (+470 nt) appears homologous to vertebrate primary processing sites; deletion of this region abolished normal pre-rRNA processing leading to 18S maturation. The downstream site (+655) corresponds to a known U3-dependent cleavage close to the 5′ end of 18S rRNA sequences (19). A 10-nt stretch of sequence complementarity containing psoralen cross-links was identified between U3 snRNA and the upstream cleavage site, consistent with hydrogen-bonded associations between RNAs. The *T. brucei* primary processing site (57) shares some sequence similarity with other primary sites, comparable to the level of identity seen between diverse species (Fig. 10A) (4). The primary cleavage region shares sequence complementarity with RNA B in sequences just downstream of the box A homology (Fig. 10B); this complementarity is analogous in position and extent to that detected between yeast U3 snRNA and cognate ETS sequences, which suggests that the 5′ region of RNA B similarly interacts with primary processing site sequences in *T. brucei*. Thus, an evolutionarily conserved interaction may bring the 5′ region of U3 snRNA, containing the well-conserved box A homology, into close proximity with the 5′ ETS primary cleavage site to somehow affect early events in pre-rRNA processing.

In general, eukaryotic rRNA maturation occurs in three steps: (i) transcription of the large primary precursor, (ii) rapid cleavage of the primary processing site in the ETS region and further cleavages to form mature 18S rRNA, and (iii) slow maturation of the 5.8S and 28S rRNAs (12). In 18S processing, the order of the cleavages which occur at the ETS/18S, 18S/ITS1, and ITS1/5.8S boundaries, as well as within ITS1, varies between organisms and even between cells within an organism. In HeLa cells, cleavage of the 18S/ITS1 boundary precedes cleavage of the ETS/18S boundary; the reverse is true of mouse, *Xenopus*, *Drosophila*, and *Saccharomyces* rRNAs (12, 19). In *T. brucei*, three predominant rRNA processing intermediates were previously identified by hybridization to cloned rDNAs (57); these intermediates correspond to the 3.7-kb ETS-18S-ITS1, 5.8-kb 5.8S-ITS2-28S, and 5.0-kb 28S pre-rRNAs; additionally, a 2.6-kb 18S-ITS1 species is reported in this work (Fig. 8). Cleavages of *T. brucei* pre-rRNAs occur close to or at the 5′ and 3′ ends of mature species except for the primary processing site in the ETS; no cleavages internal to ITS regions have been mapped (6, 57) or indicated by hybridization to ITS probes (this work). The structures of the pre-18S intermediates found in *T. brucei* suggest that the major pathway of 18S rRNA processing resembles that reported for HeLa cells; cleavage of the 18S/ITS1 boundary follows cleavage of the ETS/18S boundary.

U3 snRNA has been implicated in the primary processing event, as discussed above, and also in cleavages which lead to formation of the mature 18S rRNA. Depletion studies of yeast U3 snRNA have shown that it is required for cleavage within the 5′ ETS, at the 5′ boundary of 18S rRNA, and within ITS1 (19). In *Xenopus* cells, U3 snRNA depletion by nuclease digestion reduced cleavage of the ITS1/5.8S rRNA boundary (41). In this work, it is shown that RNA B present in deproteinized cellular extracts cosediments predominantly with the 3.7- and 2.6-kb precursors of the 18S rRNA, an interaction which can be disrupted by heat treatment, implying that RNA B associates with these pre-rRNAs through hydrogen bonding and may be involved in their processing; RNA B may affect cleavages at the boundaries of 18S rRNA with the ETS and ITS1 in addition to the primary processing event. Similarly, three yeast snRNAs that are required for processing of 35S pre-rRNA and 18S rRNA accumulation (19, 29, 48) cosediment with appropriate pre-rRNAs; U3 and snR10 RNAs are associated with the primary 35S rRNA precursor (48), and U14 snRNA is associated with 27S rRNA precursors that contain ITS1, 5.8S, ITS2, and 28S sequences (58). In addition, U14 snRNA was defined initially as 4.5S hybRNA by virtue of its ability to hybridize to 18S rRNAs from mouse and other organisms (51). In *T. brucei*, an association between RNA B and LSU rRNA precursors could not be discerned, since precursors to 5.8S and 28S rRNAs were found in a fraction that contained 18S precursors as well as RNA B. However, such an interaction would be consistent with a role for U3 snRNAs in

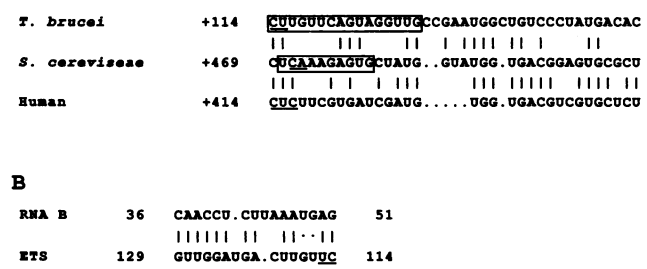

FIG. 10. (A) Sequence identity between primary processing site regions in the 5′ ETS. The *T. brucei* sequence, identified by S1 mapping and primer extension analysis at +115 from the rRNA transcription start site (57), is compared with yeast and human sequences as they were aligned in reference 4. Cleavage sites are underlined in each sequence. Regions of trypanosome and yeast ETS sequences which share complementarity with RNA B and U3 snRNA sequences are boxed. (B) Sequence complementarity between *T. brucei* RNA B sequences 3′ adjacent to the box A homology (see Fig. 1B) and the primary cleavage site region in the 5′ ETS.

separation of 18S rRNA from LSU rRNA precursors, as implied by in vivo U3 depletion studies in *Xenopus* cells (41).

This study identifies RNA B as the primary trypanosomal nucleolar U snRNA involved in rRNA processing. More nucleolar snRNAs required for ribosome biogenesis may later be recognized. Ten nucleolar snRNAs that hydrogen bond to various pre-rRNAs have been identified in yeast cells (48, 49, 58). Of these, only the U3 and U14 snRNAs are essential for growth (20, 58) and processing (18, 29) and have homologs in mammals, although rRNA processing is reduced in strains carrying snR10 gene deletions (48). In mammals, besides U3 and U14 snRNAs, the TMG-capped U8 and U13 snRNAs and the non-TMG-capped X and Y nucleolar snRNAs are found associated with fibrillarin (55). RNA B is apparently the trypanosome U3 homolog; trypanosomal counterparts to the essential U14 snRNA, as well as to other identified nucleolar snRNAs, may also exist. In addition, trypanosome-specific nucleolar snRNAs involved in removal of the five intervening sequences of the 28S pre-rRNA might be found. In this study, however, no new *T. brucei* TMG-capped snRNAs were apparent in either anti-TMG or antifibrillarin immunoprecipitates or unmasked by specific digestion of the abundant TMG-capped U2, RNA B, and U4 snRNAs. It is possible that U snRNAs of very low abundance or of relative inaccessibility to antibodies exist and were undetected by these experimental approaches. Several non-TMG-capped RNAs were present in *T. brucei* antifibrillarin immunoprecipitates and are candidates for nucleolar snRNAs involved in processing; their identities remain to be elucidated. Alternatively, it is possible that rRNA processing events require fewer nucleolar snRNAs in trypanosomes than in other organisms. At present, U3 and other snRNAs are proposed to help stabilize pre-rRNA conformations necessary for maturation (12), whereas specific nucleolar endonucleases perform the actual cleavages (44, 45). Trypanosomal pre-rRNAs may be capable of folding into conformations that can be recognized by maturases without the help of multiple nucleolar snRNAs.

ACKNOWLEDGMENTS

We thank J. Hughes, D. Tollervey, and members of the Agabian laboratory for helpful discussions. Anti-TMG cap IgG was a gift of R. Luhrmann; M. Christensen kindly provided the anti-*Physarum* fibrillarin antibody P2G3; scleroderma patient serum S4 and monoclonal antibody 72B9 were contributed by G. Reimer, K. M. Pollard, and E. M. Tan.

This work was supported by grants to N.A. from the John D. and Catherine T. MacArthur Foundation and by National Institutes of Health grant A121975.

REFERENCES

1. **Agabian, N.** 1990. *Trans* splicing of nuclear pre-mRNAs. Cell **61**:1157–1160.
2. **Aris, J. P., and G. Blobel.** 1991. cDNA cloning and sequencing of human fibrillarin, a conserved nucleolar protein recognized by autoimmone antisera. Proc. Natl. Acad. Sci. USA **88**:931–935.
3. **Baserga, S. J., X. W. Yang, and J. A. Steitz.** 1991. An intact box C sequence in the U3 snRNA is required for binding of fibrillarin, the protein common to the major family of nucleolar snRNPs. EMBO J. **10**:2645–2651.
4. **Beltrame, M., and D. Tollervey.** 1992. Identification and functional analysis of two U3 binding sites on yeast pre-ribosomal RNA. EMBO J. **11**:1531–1542.
5. **Birnstiel, M. L. (ed.).** 1988. Small nuclear ribonucleoprotein particles. Springer-Verlag KG, Berlin.
6. **Campbell, D. A., K. Kubo, C. G. Clark, and J. C. Boothroyd.** 1987. Precise identification of cleavage sites involved in the unusual processing of trypanosome ribosomal RNA. J. Mol. Biol. **196**:113–124.
7. **Christensen, M. E. (Texas A & M University).** Personal communication.
8. **Christensen, M. E., M. Jamaluddin, J. L. Swischuk, and M. E. Schelling.** 1986. Characterization of the nucleolar protein, B-36, using monoclonal antibodies. Exp. Cell Res. **166**:77–93.
9. **Craig, N., S. Kass, and B. Sollner-Webb.** 1991. Sequence organization and RNA structural motifs directing the mouse primary rRNA-processing event. Mol. Cell. Biol. **11**:458–467.
10. **Dungan, J. D., and N. Agabian (University of California at San Francisco).** Personal communication.
11. **Epstein, P., R. Reddy, and H. Busch.** 1984. Multiple states of U3 RNA in Novikoff hepatoma nucleoli. Biochemistry **23**:5421–5425.
12. **Gerbi, S. A., R. Savino, B. Stebbins-Boaz, C. Jeppesen, and R. Rivera-Leon.** 1991. A role for U3 small nuclear ribonucleoprotein in the nucleolus?, p. 452–469. *In* W. E. Hill, A. Dahlberg, R. A. Garrett, P. B. Moore, D. Schlessinger, and J. R. Warner (ed.), The ribosome: structure, function, and evolution. American Society for Microbiology, Washington, D.C.
13. **Guiltinan, M. J., M. E. Schelling, N. Z. Ehtesham, J. C. Thomas, and M. E. Christensen.** 1988. The nucleolar RNA-binding protein B-36 is highly conserved among plants. Eur. J. Cell Biol. **46**:547–553.
14. **Gutell, R. R., and G. E. Fox.** 1988. Compilation of large subunit RNA sequences presented in a structural format. Nucleic Acids Res. **16**:r175–r270.
15. **Hartshorne, T., and N. Agabian.** Unpublished data.
16. **Henriquez, R., G. Blobel, and J. P. Aris.** 1990. Isolation and sequencing of *NOP1*. A yeast gene encoding a nucleolar protein homologous to a human autoimmune antigen. J. Biol. Chem. **265**:2209–2215.
17. **Hernandez-Verdun, D.** 1991. The nucleolus today. J. Cell Sci. **99**:465–471.
18. **Hughes, J. M. X. (University of California at Santa Cruz).** Personal communication.
19. **Hughes, J. M. X., and M. Ares.** 1991. Depletion of U3 small nucleolar RNA inhibits cleavage in the 5′ external transcribed spacer of yeast pre-ribosomal RNA and impairs formation of 18S ribosomal RNA. EMBO J. **10**:4231–4239.
20. **Hughes, J. M. X., D. A. M. Konings, and G. Cesareni.** 1987. The yeast homologue of U3 snRNA. EMBO J. **6**:2145–2155.
21. **Jansen, R. P., E. C. Hurt, H. Kern, H. Lehtonen, M. Carmo-Fonseca, B. Lapeyre, and D. Tollervey.** 1991. Evolutionary conservation of the human nucleolar protein fibrillarin and its functional expression in yeast. J. Cell Biol. **113**:715–729.
22. **Jarmolowski, A., J. Zagorski, H. V. Li, and M. J. Fournier.**

1990. Identification of essential elements in U14 RNA of *Saccharomyces cerevisiae*. EMBO J. **9**:4503–4509.
23. **Jeppesen, C., B. Stebbins-Boaz, and S. A. Gerbi.** 1988. Nucleotide sequence determination and secondary structure of *Xenopus* U3 snRNA. Nucleic Acids Res. **16**:2127–2148.
24. **Kass, S., N. Craig, and B. Sollner-Webb.** 1987. Primary processing of mammalian rRNA involves two adjacent cleavages and is not species specific. Mol. Cell. Biol. **7**:2891–2898.
25. **Kass, S., K. Tyc, J. A. Steitz, and B. Sollner-Webb.** 1990. The U3 small nucleolar ribonucleoprotein functions in the first step of preribosomal RNA processing. Cell **60**:897–908.
26. **Kiss, T., and F. Solymosy.** 1990. Molecular analysis of a U3 RNA gene locus in tomato: transcription signals, the coding region, expression in transgenic tobacco plants and tandemly repeated pseudogenes. Nucleic Acids Res. **18**:1941–1949.
27. **Laird, P. W.** 1989. *Trans* splicing in trypanosomes-archaism or adaption? Trends Genet. **5**:204–208.
28. **Lapeyre, B., P. Mariottini, C. Mathieu, P. Ferrer, F. Amaldi, F. Amalric, and M. Caizergues-Ferrer.** 1990. Molecular cloning of *Xenopus* fibrillarin, a conserved U3 small nuclear ribonucleoprotein recognized by antisera from humans with autoimmune disease. Mol. Cell. Biol. **10**:430–434.
29. **Li, H. V., J. Zagorski, and M. J. Fournie.** 1990. Depletion of U14 small nuclear RNA (*snR128*) disrupts production of 18S rRNA in *Saccharomyces cerevisiae*. Mol. Cell. Biol. **10**:1145–1152.
30. **Maser, R. L., and J. P. Calvet.** 1989. U3 small nuclear RNA can be psoralen-cross-linked *in vivo* to the 5′ external transcribed spacer of pre-ribosomal-RNA. Proc. Natl. Acad. Sci. USA **86**:6523–6527.
31. **Mottram, J., K. L. Perry, R. Lizardi, R. Luhrmann, N. Agabian, and R. G. Nelson.** 1989. Isolation and sequence of four U snRNA genes of *Trypanosoma brucei brucei*: identification of the trypanosome U2, U4, and U6 RNA analogues. Mol. Cell. Biol. **9**:1212–1223.
32. **Ochs, R. L., M. A. Lischwe, W. H. Spohn, and H. Busch.** 1985. Fibrillarin: a new protein of the nucleolus identified by autoimmune sera. Biol. Cell **54**:123–134.
33. **Parker, K. A., J. P. Bruzik, and J. A. Steitz.** 1988. An *in vitro* interaction between the human U3 snRNP and 28S rRNA sequences near the α-sarcin site. Nucleic Acids Res. **16**:10493–10509.
34. **Parker, K. A., and J. A. Steitz.** 1987. Structural analysis of the human U3 ribonucleoprotein particle reveal a conserved sequence available to base pairing with pre-rRNA. Mol. Cell. Biol. **7**:2899–2913.
35. **Porter, G. L., P. L. Brennwald, K. A. Holm, and J. A. Wise.** 1988. The sequence of U3 from *Schizosaccharomyces pombe* suggests structural divergence of this snRNA between metazoans and unicellular eukaryotes. Nucleic Acids Res. **16**:10131–10151.
36. **Prestakyo, A. W., M. Tonato, and H. Busch.** 1970. Low molecular weight RNA associated with 28S nucleolar RNA. J. Mol. Biol. **47**:505–515.
37. **Puvion-Dutilleul, F., S. Mazan, M. Nicoloso, M. E. Christensen, and J. Bachellerie.** 1991. Localization of U3 RNA molecules in nucleoli of HeLa and mouse 3T3 cells by high resolution *in situ* hybridization. Eur. J. Cell Biol. **56**:178–186.
38. **Reddy, R., W.-Y. Li, D. Henning, Y. C. Choi, K. Nogha, and H. Busch.** 1981. Characterization and subcellular localization of 7-8S RNAs of Novikoff hepatoma. J. Biol. Chem. **256**:8452–8457.
39. **Reimer, G., K. M. Pollard, C. A. Penning, R. L. Ochs, M. A. Lischwe, H. Busch, and E. M. Tan.** 1987. Monoclonal autoantibody from a (New Zealand black × New Zealand white) F1 mouse and some human scleroderma sera target an Mr 34,000 nucleolar protein of the U3 RNP particle. Arthritis Rheum. **30**:793–800.
40. **Reuter, R., G. Tessars, H. Vohr, E. Gleichmann, and R. Luhrmann.** 1989. Mercuric chloride induces autoantibodies against U3 small nuclear ribonucleoprotein in susceptible mice. Proc. Natl. Acad. Sci. USA **86**:237–241.
41. **Savino, R., and S. A. Gerbi.** 1990. *In vivo* disruption of *Xenopus* U3 snRNA affects ribosomal RNA processing. EMBO J. **7**:2299–2308.
42. **Schimmang, T., D. Tollervey, H. Kern, R. Frank, and E. C. Hurt.** 1989. A yeast nucleolar protein related to mammalian fibrillarin is associated with small nucleolar RNA and is essential for viability. EMBO J. **8**:4015–4024.
43. **Selzer, P. M., P. Webster, and M. Duszenko.** 1991. Influence of Ca^{2+} depletion on cytoskeleton and nucleolus morphology in *Trypanosoma brucei*. Eur. J. Cell Biol. **56**:104–112.
44. **Shumard, C. M., and D. C. Eichler.** 1988. Ribosomal RNA processing: limited cleavages of mouse preribosomal RNA by a nucleolar endoribonuclease include the early +650 processing site. J. Biol. Chem. **263**:19346–19352.
45. **Shumard, C. M., C. Torres, and D. C. Eichler.** 1990. In vitro processing at the 3′-terminal region of pre-18S rRNA by a nucleolar endoribonuclease. Mol. Cell. Biol. **10**:3868–3872.
46. **Spencer, D. F., J. C. Collings, M. N. Schnare, and M. W. Gray.** 1987. Multiple spacer sequences in the nuclear large ribosomal RNA gene of *Crithidia fasciculata*. EMBO J. **6**:1063–1071.
47. **Stroke, I., and A. M. Weiner.** 1989. The 5′ end of U3 snRNA can be crosslinked *in vivo* to the external transcribed spacer of rat ribosomal RNA precursors. J. Mol. Biol. **210**:497–512.
48. **Tollervey, D.** 1987. A yeast small nuclear RNA is required for normal processing of pre-ribosomal RNA. EMBO J. **6**:4169–4175.
49. **Tollervey, D., and E. C. Hurt.** 1990. The role of small nucleolar ribonucleoproteins in ribosome synthesis. Mol. Biol. Rep. **14**:103–106.
50. **Tollervey, D., H. Lehtonen, M. Carmo-Fonseca, and E. C. Hurt.** 1991. The small nucleolar RNP protein NOP1 (fibrillarin) is required for pre-rRNA processing in yeast. EMBO J. **10**:573–583.
51. **Trinh-Rohlik, Q., and E. S. Maxwell.** 1988. Homologous genes for mouse 4.5S hybRNA are found in all eukaryotes and their low molecular weight RNA transcripts intermolecularly hybridize with eukaryotic 18S ribosomal RNAs. Nucleic Acids Res. **16**:6041–6055.
52. **Tschudi, C., A. R. Krainer, and E. Ullu.** 1988. The U6 RNA of *Trypansoma brucei*. Nucleic Acids Res. **16**:11375.
53. **Tschudi, C., F. F. Richards, and E. Ullu.** 1986. The U2 RNA of *Trypanosoma brucei gambiense*: implications for a splicing mechanism in trypanosomes. Nucleic Acids Res. **14**:8893–8903.
54. **Tschudi, C., and E. Ullu.** 1990. Destruction of U2, U4, or U6 small nuclear RNA blocks *trans* splicing in trypansome cells. Cell **61**:459–466.
55. **Tyc, K., and J. A. Steitz.** 1989. U3, U8 and U13 comprise a new class of mammalian snRNPs localized in the cell nucleolus. EMBO J. **8**:3113–3119.
56. **Watkins, K., T. G. Roberts, S. Michaeli, and N. Agabian. (University of California at San Francisco).** Personal communication.
57. **White, T., G. Rudenko, and P. Borst.** 1986. Three small RNAs within the 10 kb trypansome rRNA transcription unit are analogous to domain VII of other eukaryotic 28S rRNAs. Nucleic Acids Res. **14**:9471–9489.
58. **Zagorski, J., D. Tollervey, and M. L. Fournier.** 1988. Characterization of an SNR gene locus in *Saccharomyces cerevisiae* that specifies both dispensible and essential small nuclear RNAs. Mol. Cell. Biol. **8**:3282–3290.